Protein Ionization

Deutsche Ausgabe: DOI: 10.1002/ange.201605335
Internationale Ausgabe: DOI: 10.1002/anie.201605335

Multiple Ionization of Free Ubiquitin Molecular Ions in Extreme Ultraviolet Free-Electron Laser Pulses

Thomas Schlathölter, Geert Reitsma, Dmitrii Egorov, Olmo Gonzalez-Magaña, Sadia Bari, Leon Boschman, Erwin Bodewits, Kirsten Schnorr, Georg Schmid, Claus Dieter Schröter, Robert Moshammer, and Ronnie Hoekstra*

Abstract: *The fragmentation of free tenfold protonated ubiquitin in intense 70 femtosecond pulses of 90 eV photons from the FLASH facility was investigated. Mass spectrometric investigation of the fragment cations produced after removal of many electrons revealed fragmentation predominantly into immonium ions and related ions, with yields increasing linearly with intensity. Ionization clearly triggers a localized molecular response that occurs before the excitation energy equilibrates. Consistent with this interpretation, the effect is almost unaffected by the charge state, as fragmentation of sixfold deprotonated ubiquitin leads to a very similar fragmentation pattern. Ubiquitin responds to EUV multiphoton ionization as an ensemble of small peptides.*

The investigation of complex biological molecules by means of scattering or absorption of energetic photons from high-brilliance light sources is a very powerful approach to address the molecules' chemical and electronic structure and dynamics. Established techniques such as X-ray photoelectron spectroscopy (XPS) or near-edge X-ray absorption fine structure (NEXAFS) spectroscopy involve small absorption cross sections that usually dictate the use of dense condensed-phase targets.[1,2] Soft X-ray spectroscopy has successfully been used for protein identification and mapping.[3,4] However, in the condensed phase, structural and dynamic molecular properties are often strongly influenced by intermolecular interactions such as ultrafast energy transfer[5] or the inevitable radiation damage.[6,7] With the promise held by ultrabright X-ray free-electron lasers (FEL), of imaging before destruction, it is crucial to establish how (and also how fast) single gas-phase or nanocrystalline biomolecular systems respond to simultaneous absorption of many energetic photons.[8] Pioneering experiments proved the feasibility of femtosecond (fs) X-ray FEL diffraction imaging of biomolecular nanocrystals in a liquid jet, indicating that photodestruction proceeds slower than the imaging process.[9,10] It is still under debate whether this pathway is also valid for single free proteins. Experimental studies on the response of single proteins to fs energetic photon pulses are thus called for.

Mass spectrometric techniques that combine electrospray ionization (ESI) and radiofrequency (RF) ion traps have recently been introduced for the investigation of photoionization dynamics in gas-phase protein ions. The first soft X-ray photoionization studies at the C, N, and O K-edges were performed on ninefold protonated cytochrome c (104 amino acid residues).[11] Mainly nondissociative single and double ionization was observed, with spectral features similar to the NEXAFS data from solid protein films. Protein backbone scission was very weak and only CO_2 loss appeared as an additional dissociation channel. The predominance of non-dissociative processes is remarkable, because core ionization/excitation leads to substantial local excitation. In contrast, soft X-ray photoionization of the small gas-phase protonated leucine enkephalin (five residues) leads almost exclusively to extensive fragmentation.[12] Here, small sidechain-related fragments dominate the breakup pattern. These findings can be understood in the context of ionization-induced fast dissociation through repulsive states before internal vibrational redistribution (IVR) of the excitation energy.[13] Vacuum ultraviolet (VUV) photoionization studies on a series of synthetic protonated peptides of variable size (2–12 residues) confirmed this scenario.[14] From these measurements, it was determined that ionization along the peptide backbone followed by fast charge migration towards an aromatic sidechain is the main underlying process. VUV photoionization of larger multiply protonated proteins such as cytochrome c leads almost exclusively to nondissociative ionization.[15]

Why is fast sidechain loss suppressed in larger systems, even though it is thought to occur before IVR happens? What is the role of the photoinduced charge(s)? To answer these questions, we systematically investigated multiple ionization

[*] Dr. T. Schlathölter, Dr. G. Reitsma, D. Egorov, Dr. O. Gonzalez-Magaña, L. Boschman, Dr. E. Bodewits, Prof. Dr. R. Hoekstra
Zernike Institute for Advanced Materials, University of Groningen
Nijenborgh 4, 9747 AG Groningen (The Netherlands)
E-mail: t.a.schlatholter@rug.nl
Dr. G. Reitsma
Max-Born-Institute
Max Born Strasse 2A, 12489 Berlin (Germany)
Dr. S. Bari
European XFEL GmbH
Holzkoppel 4, 22869 Schenefeld (Germany)
L. Boschman
Kapteyn Institute
Landleven 12, 9747 AD Groningen (The Netherlands)
Dr. K. Schnorr, G. Schmid, Dr. C. D. Schröter, Dr. R. Moshammer
Max-Planck-Institut für Kernphysik
Saupfercheckweg 1, 69117 Heidelberg (Germany)
Dr. S. Bari
DESY, Notkestraße 85, 22607 Hamburg (Germany)
Supporting information and the ORCID identification number(s) for the author(s) of this article can be found under http://dx.doi.org/10.1002/anie.201605335.

of tenfold protonated ubiquitin $[ubi+10H]^{10+}$ ($m = 8565$ u, 76 amino acid residues) in extreme ultraviolet (EUV) fs pulses from the FEL FLASH.[16] Ubiquitin has no disulfide bridges and its tertiary structure is thus not very rigid. Tenfold protonation is known to induce substantial structural relaxation driven by Coulomb repulsion of the protonation sites.[15] The gas-phase conformation of $[ubi+10H]^{10+}$ can be classified as elongated (with maximum elongation reached for 13-fold protonation).[17] Charge or energy transport upon photoabsorption in this system therefore most likely proceeds solely along the protein backbone.

The experiments were performed by interfacing a home-built tandem mass spectrometer with beamlines at the FEL FLASH (DESY, Hamburg, Germany) and the synchrotron facilities BESSY II (HZB, Berlin, Germany) and MAXII (Maxlab, Lund, Sweden; see the Supporting Information for details).

A typical mass spectrum of $[ubi+10H]^{10+}$ products after interaction with 70 fs FEL pulses of 90 eV photons is shown in Figure 1. The pulse energies were attenuated to 0.1 μJ for

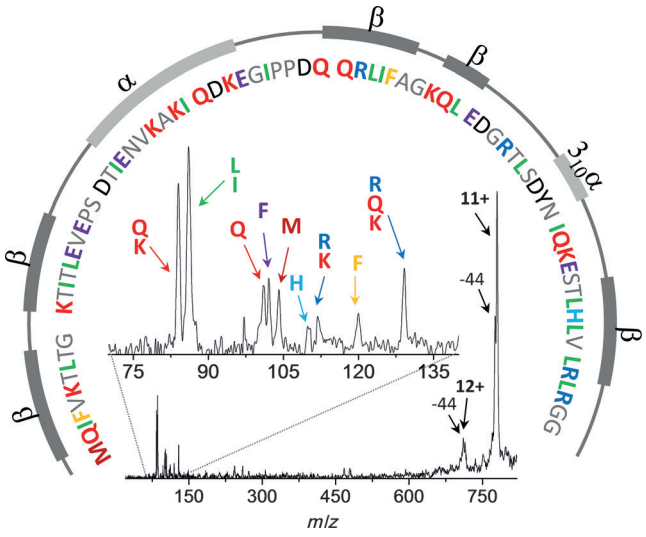

Figure 1. One-letter-code sequence of ubiquitin (colored letters) and secondary structure (β-sheets and α-helices) and mass spectrum (lower spectrum) for $[ubi+10H]^{10+}$ photoionization by 0.1 μJ 70 fs EUV pulses at 90 eV. Inset: Expansion of the region for immonium ion related fragments.

single photon absorption conditions. As seen previously for soft X-ray[11] and VUV single photon absorption[15] of gas-phase protonated proteins, nondissociative single ionization into $[ubi+10H]^{11+}$ (labeled 11+) is the dominant process, in part accompanied by CO_2 loss ($m = 44$, labelled −44). Other large fragment channels are weak. Nondissociative double ionization (labeled: 12+) and associated CO_2 loss are significantly weaker. In the range between the trap cut-off (m/z ca. 75) and m/z 150, a group of peaks shows up with intensities exceeding those of $[ubi+10H]^{12+}$. Almost all these peaks can be assigned to immonium (related) ions (internal fragments containing a single sidechain formed by two adjacent backbone cleavages). This result is consistent with our previous VUV photoionization studies on much smaller singly protonated peptides.[13,14] Ubiquitin primary and secondary structures are shown in the circle around the spectrum. The one-letter codes are also used to label the immonium peaks. Amino acids observed in the spectrum are labeled in color and those not observed are shown in black. Amino acids outside the mass range of the system are shown in gray.

Most amino acids contribute to the immonium peaks but their relative intensities do not reflect the amino acid molar ratio of ubiquitin. For instance, the *L*eucine/*I*soleucine peak ($m = 86$, 16 out of 76 residues) is only four times stronger than the *M*ethionine peak ($m = 104$, 1 residue), since just a single backbone scission is required for immonium formation from the NH_2 terminal M.

In Figure 2, the same mass spectrum (Figure 2a) is compared to five photoionization mass spectra obtained under other conditions. All spectra have been normalized to the total photoabsorption cross section at the respective photon energy to suppress cross-sectional effects. An EUV single-photon absorption reference spectrum obtained with synchrotron radiation of 90 eV (Figure 2d) shows features qualitatively and quantitatively similar to the 0.1 μJ FEL spectrum at $h\nu = 90$ eV (Figure 2a), albeit on a 30% lower relative intensity scale. At lower photon energy (45 eV, Figure 2c), single-photon conditions induce slightly less double ionization and fragmentation. At 45 eV, only about 25% of the photoabsorption involves strongly bound atomic 2s electrons. At 90 eV, this fraction increases to 45%.[18] As a consequence, excitation energies are on average markedly higher.

For resonant C 1s–π^* excitation at $h\nu = 288.5$ eV (Figure 2e) subsequent Auger electron emission is the main ionization mechanism. Again, the mass spectrum resembles the low-intensity FEL spectrum (Figure 2a), albeit with lower overall intensities. Single-photon C core ionization at 310 eV (Figure 2f) followed by Auger ionization leads to two-electron removal. From Figure 2f, it is evident that the $[ubi+10H]^{12+}$ peak is more intense than $[ubi+10H]^{11+}$ peak, which is strongly suppressed.

For massive multiphoton absorption in 2.3 μJ, 70 fs FEL pulses (Figure 2b) immonium related fragment ions with small m/z values dominate the spectrum. Their distribution is very similar to the one at 0.1 μJ (Figure 2a). The $[ubi+10H]^{11+}$ and $[ubi+10H]^{12+}$ peaks remain visible. These ions cannot be formed in the focus of the beam, where single and double photoabsorption conditions are ruled out, considering the orders of magnitude of photon fluence and photoabsorption cross section. Accordingly, $[ubi+10H]^{11+}$ and $[ubi+10H]^{12+}$ are most likely formed in the low-intensity halo surrounding the high-intensity focus of the beam.

It is instructive to quantitatively analyze partial ion yields as a function of FEL pulse intensity. The spatial beam profile perpendicular to the beam axis is approximately Gaussian, and the (time averaged) intensity profile around the focus can thus be described as:[19]

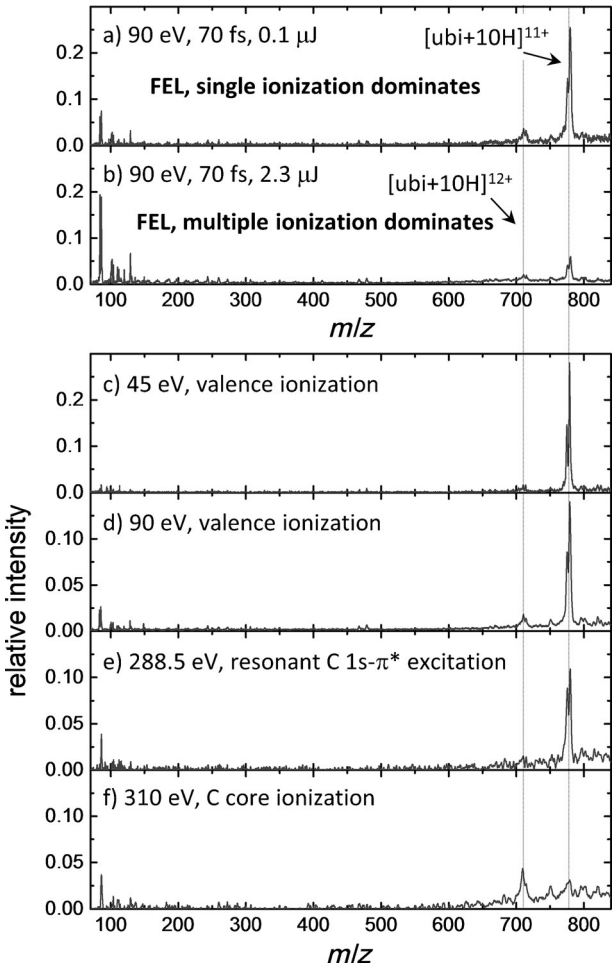

Figure 2. Photoionization mass spectra of $[ubi+10H]^{10+}$ in 70 fs EUV pulses at 90 eV at 0.1 μJ (a) and at 2.3 μJ (b) pulse energy. For comparison, data for single photon absorption (obtained at the BESSY II synchrotron) at 45 eV (c), 90 eV (d), 288.5 eV (e), and 310 eV (f) are shown. The intensities are normalized to the respective total photoabsorption cross section.

$$I(r,z) = \frac{4ln2}{\pi\Delta^2(z)}\exp(-\frac{4ln2}{\Delta^2(z)}r^2)I_0 \text{ with } \Delta(z) = \Delta_0\sqrt{1+\left(\frac{z}{z_0}\right)^2} \qquad (1)$$

with $\Delta(z)$ the beam width at a distance z from the focus and r the radial distance from the beam axis. The Gaussian width of the beam in the focus (beam waist) is $\Delta_0 = 25$ μm and the Rayleigh length (representing beam divergence) is $z_0 =$ 0.84 mm. Details are given in the Supporting Information.

The estimation of photoabsorption yields by using this equation requires the ubiquitin photoabsorption cross section at 90 eV. This photon energy well exceeds the binding energy of the deepest O 2s valence orbitals (34.3 eV in glycylglycine[20]). The $[ubi+10H]^{10+}$ ionization energy can be extrapolated from the value for $[ubi+9H]^{9+}$ (ca. 13.9 eV)[15] to be 14.2 eV. Well above the ionization threshold, photoionization cross sections are usually reproduced within a few percent by summation of the atomic cross sections.[21] For ubiquitin (378 C, 105 N, 118 O, 1 S, 629 H atoms), a total cross section $\sigma_{total}(90\text{ eV})$ of approximately 6.7×10^{-18} cm^2 is obtained when using tabulated atomic data.[18]

With $I(r,z)$ and σ_{total}, the mean ionization state of ubiquitin cations in the focus of an FEL pulse can be determined for every space coordinate, assuming independent photoabsorption events with identical cross sections. This assumption is based on 1) the moderate FEL intensity that leads to only relatively few ionization events per ubiquitin cation and 2) the small increase in protein ionization potential with charge state that typically amounts to less than 1 eV per charge state, even when structural relaxation is hampered.[15] Assuming Poisson distributed ionization states, the distribution of the degrees of photoionization in the total focal volume, is obtained by mere integration.

Figure 3a displays the experimental total photoionization yield ($[ubi+10H]^{10+}$ loss from the trap) as a function of FEL

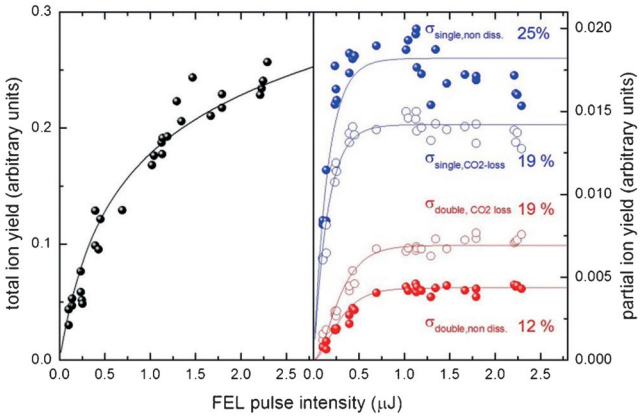

Figure 3. a) Total ion photoionization yield as a function of FEL pulse intensity and b) nondissociative single ionization ($[ubi+10H]^{11+}$ and $[ubi+10H-CO_2]^{11+}$) (blue) and nondissociative double ionization ($[ubi+10H]^{12+}$ and $[ubi+10H-CO_2]^{12+}$) (red). The symbols represent experimental data and the lines have been calculated using Equation (1) for a focus fwhm of 25 μm (see text).

pulse intensity in arbitrary units. The calculated total yield was scaled to fit the experimental data. Figure 3b shows partial ion yields for nondissociative single and double ionization, and for the associated CO_2 loss channels. For comparison, the calculated yields for one and two photon absorption, respectively are given as solid lines (data scaled with the same factor as for the total yield and with a branching ratio obtained by scaling). For single ionization, the branching ratios of 25 % for the nondissociative channel ($[ubi+10H]^{11+}$) and 19 % for additional CO_2 loss ($[ubi+10H-CO_2]^{11+}$) are found. The remaining 56 % is likely to give rise to unresolved fragmentation channels in the extended pedestal of the single-ionization peaks (see also Figure 1, inset). For double ionization, the branching ratios of 12 % ($[ubi+10H]^{12+}$) and 19 % ($[ubi+10H-CO_2]^{12+}$) are substantially lower because the increased excitation energy accompanying the ionization process induces stronger fragmentation. Nondissociative triple ionization is not observed. We have only considered independent single photoionization processes here. It is known that for $h\nu = 90$ eV, double photoionization contributes significantly (e.g. about 20 % for benzene),[22] partly because of direct simultaneous emission of two electrons and

partly because of sequential processes via excited singly charged intermediates.

The increase of single and double ionization yields with pulse intensity is due to the increase of the ionization volume. However, our main interest is multiple ionization in very strong EUV fields. The calculations (see the Supporting Information) show that the distribution of ionization states reached in the beam focus shifts dramatically with beam intensity. At 0.1 μJ pulse energy, about 97% of the ion signal is due to single ionization, while at 2.3 μJ, much higher initial charge states are formed, as the model for instance predicts that 1% of the photoionized proteins underwent 18-fold ionization. The bimodal nature of the spectrum in Figure 2b (2.3 μJ) resembles the superposition of two distinct photoionization regimes identified in gas-phase synchrotron experiments: 1) nondissociative single and double ionization[11] for protonated large proteins, and 2) fragmentation, with immonium ions dominating,[12,13] for smaller protonated peptides. The peaks in the low-*m/z* part of the spectrum (immonium ions) have high intensities, thus indicating that the low-*m/z* ions are related to multiple-photon absorption processes in the high-intensity part of the focus.

Before investigating this phenomenon in more detail, it is important to demonstrate that it is not limited to a small range of protein charge states. To this end, photoabsorption in a multiply deprotonated system $[ubi-6H]^{6-}$ was studied. The obtained mass spectra are displayed in Figure 4. Absorption

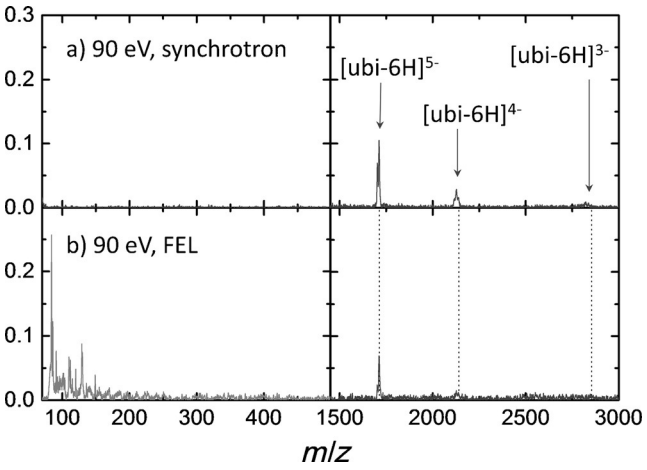

Figure 4. Photoionization mass spectra of $[ubi-6H]^{6-}$ under single 90 eV photon conditions (a) (obtained at the BESSY II synchrotron) and for 90 fs EUV pulses at 90 eV at 8.5 μJ (b). The intensities are normalized to the respective total photoabsorption cross section. In both cases, no small negative fragment ions are observed. The low mass spectrum in (b) represents positive fragment ions formed from the negative precursor $[ubi-6H]^{6-}$.

of a single 90 eV photon leads to nondissociative detachment of one or more electrons, that is, formation of $[ubi-6H]^{5-}$, $[ubi-6H]^{4-}$, and $[ubi-6H]^{3-}$ (see Figure 4a, right panel). The peaks are broadened because of the loss of small neutral groups, as also observed for $[ubi+10H]^{10+}$. The high *m/z* value of $[ubi-6H]^{2-}$ (not shown here) prevents unambiguous identification because of low detection efficiency and strong broadening of the peak. No negative small-fragment ions are observed (see Figure 4a, left panel).

For the case of intense FEL pulses, electron detachment into $[ubi-6H]^{5-/4-/3-}$ remains an important channel (see Figure 4b, right panel), analogous to the case of $[ubi+10H]^{10+}$, where nondissociative ionization into $[ubi+10H]^{11+/12+}$ was still observed for 70 fs and 2.3 μJ pulses (see Figure 2b), and also for $[ubi-6H]^{6-}$ in slightly more intense FEL pulses (90 fs and 8.5 μJ). As for single-photon absorption, small negative fragments are unobserved (data not shown, here). However, Figure 4b (left panel) displays the positive-ion mass spectrum for the lower mass range. The mass spectrum is qualitatively and quantitatively very similar to that obtained from $[ubi+10H]^{10+}$ (Figure 2b), with immonium ions as dominating features. Sequence ions, which arise solely from backbone scission are almost completely absent. If addition of 16 negative charges to a single ubiquitin molecular ion does not have a substantial influence on ubiquitin photofragmentation in intense EUV pulses, fragmentation resulting from Coulomb repulsion can be ruled out.

Immonium (or related) ions are representative for the low *m/z* part of the spectrum, and the yields for four such ions as a function of FEL pulse intensity are shown in Figure 5, where

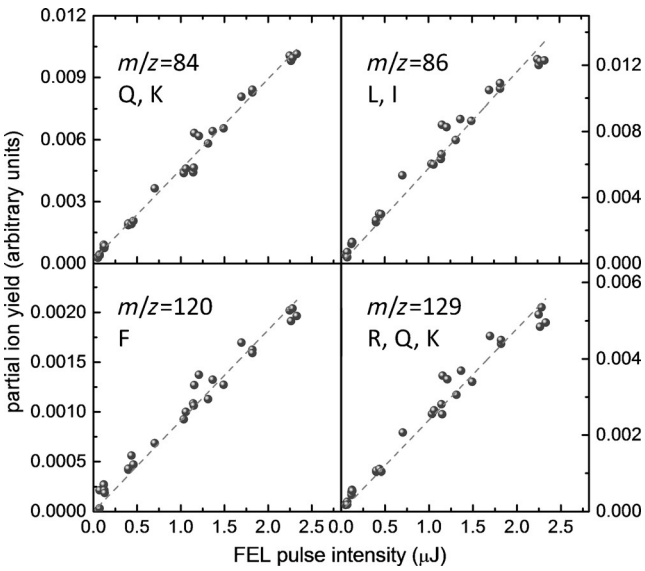

Figure 5. Partial ion yields as a function of photons per micropulse for four of the strongest immonium (and related) ions. The scaling is identical to Figure 3. The other immonium ions also follow a linear dependence.

a clear linear dependence is observed (as for the other immonium ions). This behavior is clearly different from the total ion yield (Figure 3a) and in particular from the partial yields for nondissociative single and double ionization, which saturate at moderate photon fluxes (Figure 3b). The bimodal nature of the mass spectrum (high *m/z* peaks, mainly arising from nondissociative photoionization processes and low *m/z* peaks, mainly from immonium ions) persists when the pulse intensity increases. Relatively more immonium ions are

formed and relatively less nondissociative processes occur, but there is no transition region in which intermediate-size fragments that arise from backbone scission of the protein (sequence ions) prevail. Both findings suggest that fs EUV multiphoton ionization cannot be viewed as a process in which the number of increased photons translates into a gradual increase of protein total internal energy and charge, ultimately emerging in the fragmentation pattern. The correct scenario seems to be one in which the protein undergoes independent photoionization processes. Each local photoionization process then induces fast local fragmentation processes in which immonium ions are produced. These processes occur before IVR can set in. The protein thus responds to EUV photoionization, as an ensemble of small, few amino acid peptides.

We have shown that fs absorption of ten or more EUV photons by a small protein induces fragmentation into small fragments, independent on the initial charge state of the protein. The molecular dynamics are dominated by fast local structural responses. In the future, these processes will be studied in more detail by pump–probe type experiments and for the even higher intensities and photon energies, employed in hard X-ray diffraction imaging.

Acknowledgements

The FEL experiments were carried out at the FLASH facility at DESY, a member of the Helmholtz Association (HGF). We would like to thank Stefan Düsterer for assistance in using beamline BL3. We also thank the Helmholtz Zentrum Berlin for allocation of synchrotron beamtime and acknowledge funding from the EC's Seventh Framework Programme (FP7/2007–2013, grant no. 312284). G.R. is supported by the Netherlands Organization for Scientific Research (NWO, Rubicon 68-50-1410).

Keywords: free-electron lasers · mass spectrometry · multiphoton ionization · photoionization · proteins

How to cite: *Angew. Chem. Int. Ed.* **2016**, *55*, 10741–10745
Angew. Chem. **2016**, *128*, 10899–10903

[1] G. Hähner, *Chem. Soc. Rev.* **2006**, *35*, 1244.
[2] K. M. Lange, E. F. Aziz, *Chem. Soc. Rev.* **2013**, *42*, 6840–6859.
[3] J. Stewart-Ornstein, A. P. Hitchcock, D. H. Cruz, P. Henklein, J. Overhage, K. Hilpert, J. D. Hale, R. E. W. Hancock, *J. Phys. Chem. B* **2007**, *111*, 7691–7699.
[4] Y. Zubavichus, A. Shaporenko, M. Grunze, M. Zharnikov, *J. Phys. Chem. B* **2008**, *112*, 4478–4480.
[5] T. Jahnke, H. Sann, T. Havermeier, K. Kreidi, C. Stuck, M. Meckel, M. Schöffler, N. Neumann, R. Wallauer, S. Voss, A. Czasch, O. Jagutzki, A. Malakzadeh, T. Weber, F. Afaneh, H. Schmidt-Böcking, R. Dörner, *Nat. Phys.* **2010**, *6*, 139.
[6] F. Kaneko, M. Tanaka, S. Narita, T. Kitada, T. Matsui, K. Nakagawa, A. Agui, K. Fujii, A. Yokoya, *J. Electron Spectrosc. Relat. Phenom.* **2005**, *144*, 291–294.
[7] S. Ptasinska, A. Stypczynska, T. Nixon, N. J. Mason, D. V. Klyachko, L. Sanche, *J. Chem. Phys.* **2008**, *129*, 065102.
[8] R. Neutze, R. Wouts, D. v. d. Spoel, E. Weckert, J. Hajdu, *Nature* **2000**, *406*, 752.
[9] H. N. Chapman, P. Fromme, A. Barty, T. A. White, R. A. Kirian, A. Aquila, M. S. Hunter, J. Schulz, D. P. DePonte, U. Weierstall, R. B. Doak, F. R. N. C. Maia, A. V. Martin, I. Schlichting, L. Lomb, N. Coppola, R. L. Shoeman, S. W. Epp, R. Hartmann, D. Rolles, A. Rudenko, L. Foucar, N. Kimmel, G. Weidenspointner, P. Holl, M. Liang, M. Barthelmess, C. Caleman, S. Boutet, M. J. Bogan, J. Krzywinski, C. Bostedt, S. Bajt, L. Gumprecht, B. Rudek, B. Erk, C. Schmidt, A. Hoemke, C. Reich, D. Pietschner, L. Strueder, G. Hauser, H. Gorke, J. Ullrich, S. Herrmann, G. Schaller, F. Schopper, H. Soltau, K. Kuehnel, M. Messerschmidt, J. D. Bozek, S. P. Hau-Riege, M. Frank, C. Y. Hampton, R. G. Sierra, D. Starodub, G. J. Williams, J. Hajdu, N. Timneanu, M. M. Seibert, J. Andreasson, A. Rocker, O. Joensson, M. Svenda, S. Stern, K. Nass, R. Andritschke, C.-D. Schroter, F. Krasniqi, M. Bott, K. E. Schmidt, X. Wang, I. Grotjohann, J. M. Holton, T. R. M. Barends, R. Neutze, S. Marchesini, R. Fromme, S. Schorb, D. Rupp, M. Adolph, T. Gorkhover, I. Andersson, H. Hirsemann, G. Potdevin, H. Graafsma, B. Nilsson, J. C. H. Spence, *Nature* **2011**, *470*, 73-U81.
[10] I. Schlichting, J. Miao, *Curr. Opin. Struct. Biol.* **2012**, *22*, 613.
[11] A. R. Milosavljević, F. Canon, C. Nicolas, C. Miron, L. Nahon, A. Giuliani, *J. Phys. Chem. Lett.* **2012**, *3*, 1191–1196.
[12] O. González-Magaña, G. Reitsma, M. Tiemens, L. Boschman, R. Hoekstra, T. Schlathölter, *J. Phys. Chem. A* **2012**, *116*, 10745.
[13] S. Bari, O. Gonzalez-Magaña, G. Reitsma, R. Hoekstra, J. Werner, S. Schippers, T. Schlathölter, *J. Chem. Phys.* **2011**, *134*, 024314.
[14] O. González-Magaña, G. Reitsma, S. Bari, R. Hoekstra, T. Schlathölter, *Phys. Chem. Chem. Phys.* **2012**, *14*, 4351–4354.
[15] A. Giuliani, A. R. Milosavljević, K. Hinsen, F. Canon, C. Nicolas, M. Refregiers, L. Nahon, *Angew. Chem. Int. Ed.* **2012**, *51*, 9552; *Angew. Chem.* **2012**, *124*, 9690.
[16] K. Tiedtke, A. Azima, N. von Bargen, L. Bittner, S. Bonfigt, S. Duesterer, B. Faatz, U. Fruehling, M. Gensch, C. Gerth, N. Guerassimova, U. Hahn, T. Hans, M. Hesse, K. Honkavaar, U. Jastrow, P. Juranic, S. Kapitzki, B. Keitel, T. Kracht, M. Kuhlmann, W. B. Li, M. Martins, T. Nunez, E. Ploenjes, H. Redlin, E. L. Saldin, E. A. Schneidmiller, J. R. Schneider, S. Schreiber, N. Stojanovic, F. Tavella, S. Toleikis, R. Treusch, H. Weigelt, M. Wellhoefer, H. Wabnitz, M. V. Yurkov, J. Feldhaus, *New J. Phys.* **2009**, *11*, 023029.
[17] S. L. Koeniger, D. E. Clemmer, *J. Am. Soc. Mass Spectrom.* **2007**, *18*, 322–331.
[18] J. J. Yeh, *Atomic Calculation of Photoionization Cross-Sections and Asymmetry Parameters*, Gordon and Breach, Langhorne, **1993**.
[19] R. Santra, C. H. Greene, *Phys. Rev. A* **2004**, *70*, 053401.
[20] V. Feyer, O. Plekan, R. Richter, M. Coreno, K. C. Prince, V. Carravetta, *J. Phys. Chem. A* **2009**, *113*, 10726–10733.
[21] R. Feng, G. Cooper, C. E. Brion, *J. Electron Spectrosc. Relat. Phenom.* **2002**, *123*, 199.
[22] K. Jänkälä, P. Lablanquie, F. Penent, J. Palaudoux, L. Andric, M. Huttula, *Phys. Rev. Lett.* **2014**, *112*, 143005.

Received: June 1, 2016
Published online: July 25, 2016

